v. 4, n. 25, 2024

Journal of Engineering Research

CHITOSAN AS A GREEN CORROSION INHIBITOR FOR CARBON STEEL: PHYSICAL-CHEMICAL AND ELECTROCHEMICAL CHARACTERIZATION

Acceptance date: 22/10/2024
Submission date: 08/10/2024

Guilherme Kusler Possani
Post-graduate Program in Mining, Metallurgy and Materials Engineering (PPGE3M), Federal University of Rio Grande do Sul (UFRGS), Porto Alegre, RS, Brazil
http://lattes.cnpq.br/1835365473390795

João Pedro Camargo Santos
Metallurgy Engineering, Federal University of Rio Grande do Sul (UFRGS), Porto Alegre, RS, Brazil
http://lattes.cnpq.br/1265647058706915

Eduardo Luis Schneider
Post-graduate Program in Mining, Metallurgy and Materials Engineering (PPGE3M), Federal University of Rio Grande do Sul (UFRGS), Porto Alegre, RS, Brazil
http://lattes.cnpq.br/4086393631403899

Lisete Cristine Scienza
Post-graduate Program in Mining, Metallurgy and Materials Engineering (PPGE3M), Federal University of Rio Grande do Sul (UFRGS), Porto Alegre, RS, Brazil
http://lattes.cnpq.br/5146642075973511

All content in this magazine is licensed under a Creative Commons Attribution License. Attribution-Non-Commercial-Non-Derivatives 4.0 International (CC BY-NC-ND 4.0).

Abstract: Some natural polymers, such as chitosan, have emerged as promising corrosion inhibitors for metals due to their ability to form complexes with metal ions and create a protective barrier on metal surfaces. In this study, a commercial chitosan was characterized using techniques such as X-ray diffraction (XRD), Fourier-transform infrared spectroscopy (FT-IR), and thermogravimetric analysis (TGA), and its performance as a corrosion inhibitor was evaluated using potentiodynamic polarization (PP) and electrochemical impedance spectroscopy (EIS). The physicochemical characterization revealed mineral impurities and thermal degradation above 280°C, which could limit its use in certain industrial systems. Electrochemical tests showed that as the chitosan concentration increased, the corrosion potential (Ecorr) shifted to a more noble value and the charge transfer resistance also increased. Chitosan effectively inhibited carbon steel corrosion in an acidic sodium chloride solution, achieving an inhibition efficiency of over 70% at 800 ppm, highlighting its potential as a sustainable solution for mitigating corrosion.
Keywords: Chitosan, green corrosion inhibitor, corrosion, carbon steel.

INTRODUCTION

Carbon steel is the most widely used metal in industries due to its favorable properties and cost-effectiveness. However, like other oxidizable metals, it has low resistance to corrosion, especially in acidic and alkaline environments (Oyekunle et al., 2019). Corrosion control is critical from technical, economic, environmental, and aesthetic perspectives, and the use of inhibitors is one of the most effective methods for protecting metals from corrosion (Arthur et al., 2013).

A corrosion inhibitor is a substance that, when added in small concentrations to an environment, effectively reduces the corrosion rate of metals exposed to that environment. Traditional inhibitors, however, are often expensive, toxic, and environmentally harmful. As a result, cost, health concerns, and environmental regulations have driven researchers to explore natural products as "green corrosion inhibitors" (Raja et al., 2013; Ashassi-Sorkhabi & Kazempour, 2020). These compounds are gaining interest due to their safety, biodegradability, cost-effectiveness, eco-friendliness (no heavy metals or toxic compounds), and renewability. Examples include amino acids, alkaloids, polyphenols and plant extracts, often derived from agro-industrial by-products and agricultural residues (Marzorati et al., 2019).

Polar compounds containing oxygen, sulfur, and nitrogen, as well as non-polar compounds with aromatic rings, aliphatic chains, heterocyclic rings, or functional groups, can effectively adsorb to metal surfaces. The complexes formed with metal ions cover the surface, shielding the metal from corrosive agents. In general, inhibitor performance depends on factors such as the metal's surface charge, adsorption mechanism, chemical structure, concentration, solution pH, exposure time, and temperature (Elshamy et al., 2017; Hossain et al., 2020).

Chitosan, is a biodegradable polysaccharide derived from the deacetylation of chitin, which is naturally found in the shells of shrimp, lobsters, and crabs, as well as in fungal cell walls and insect cuticles, has shown promise as a corrosion inhibitor (Atta et al., 2015; Rabizadeh & AsI, 2018; Pellis et al., 2022). Its structure (Figure 1) consists of N-glucosamine and N-acetyl-glucosamine units linked by β-1,4 glucosidic bonds. Due to its biocompatibility, biodegradability, non-toxicity, and antimicrobial properties, chitosan is widely used in various fields (Du & Vuong, 2019; Verma et al., 2018). The presence of oxygen and nitrogen atoms in its structure makes chitosan

a potential metal corrosion inhibitor. Its anti-corrosive properties have been evaluated for steel alloys (Ashassi-Sorkhabi & Kazempour, 2020; Zhang et al., 2023; Hasanin & Al Kley, 2023; Kumar et al., 2024; Farag et al., 2024), aluminum (Carneiro et al., 2015; Lai et al., 2021), and copper in acidic environments (Umoren & Solomon, 2014; Solomon et al., 2017). According to Fayomi et al. (2018), the corrosion capacity of chitosan is a function of its molecular structure, where its electron-rich amino and hydroxyl groups are capable of forming bonds on the surface of metals, resulting in protection against corrosion through coordinated bonds, as that these electrons are distributed freely to the empty or partially occupied iron orbitals.

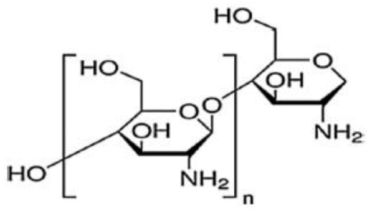

Figure 1 - Molecular structure of chitosan (Solomon et al., 2017)

The effectiveness of corrosion inhibitors depends on several factors, and a detailed study is required to select the appropriate inhibitor for a specific system. In this study, X-ray diffraction (XRD), Fourier-transform infrared spectroscopy (FT-IR), thermogravimetric analysis (TGA), potentiodynamic polarization (PP), and electrochemical impedance spectroscopy (EIS) were employed to characterize chitosan for its potential use in the anticorrosive protection of carbon steel in an aqueous acidic sodium chloride solution.

EXPERIMENTAL

MATERIALS AND SAMPLE PREPARATION

Chitosan, derived from crustacean shells, was commercially purchased and used without any further purification. Other chemicals, including NaOH, NaCl, and ethyl alcohol, were of analytical grade.

Cold-rolled carbon steel sheets measuring 0.9 x 1200 mm were used as specimens for the electrochemical experiments. According to supplier data, their chemical composition (in wt%) is as follows: 0.0662% C, 0.0070% Si, 0.3420% Mn, 0.0160% P, 0.0081% S, 0.0370% Al, and 0.010% Mo. Prior to the electrochemical testing, the specimens underwent a surface cleaning procedure (steps 1 to 8) as outlined in Table 1.

Step	Procedure	Parameter
1	Sandpaper (SiC)	120, 320, 600, 1200, 2000 #
2	Washing	Deionised water
3	Ultrasonic degreaser	Ethanol, 1 min
4	Alkaline degreaser	35 g/L NaOH + 1 g/L lauril sodium sulphate, 5 min, 80 °C
5	Washing	Deionised water
6	Acid pickling	5% (v/v) H_2SO_4, 10 min
7	Washing	Deionised water
8	Drying	Cold air stream

Table 1 - Procedures and parameters of sample preparation.

PHYSICAL-CHEMICAL CHARACTERIZATION

X-ray diffraction (XRD) measurements were performed using a Siemens (BRUKER AXS) D-5000 X-ray diffractometer, equipped with an in-beam curved graphite monochromator, operating at 40 kV/30 mA (CuKα radiation = 1.5406 Å). The scan range was from 6° to 60° (2θ), with a step size of 0.05°s^{-1}, divergence and anti-scattering slits set at 1°, and a reception slit of 0.6 mm.

Fourier-transform infrared spectroscopy (FT-IR) was conducted using a Shimadzu IR Affinity-1 FT-IR spectrometer with a resolution of 4 cm^{-1}, covering a range from 4000 cm^{-1} to 400 cm^{-1}, with 10 scans. Samples were analyzed in powder form (1 part sample to 5 parts KBr) using the attenuated total reflectance (ATR) technique.

The thermal properties of chitosan were analyzed using thermogravimetric analysis (TGA) and derivative thermogravimetry (DTG) techniques on a Perkin-Elmer TGA 4000 thermobalance. The analysis was conducted from 20°C to 800°C with a heating rate of 10°C min^{-1} under a nitrogen atmosphere.

ELECTROCHEMICAL ANALYSIS

Chitosan was added to a 0.1 M NaCl solution (pH 3.5 ± 0.2) at concentrations of 400 ppm and 800 ppm. Electrochemical experiments were conducted using a Metrohm DropSens 400is Potentiostat/Galvanostat connected to the Drop View software, at room temperature and under naturally aerated conditions. A platinum wire was used as the counter electrode (CE), an Ag/AgCl electrode as the reference electrode (RE), and the specimen served as the working electrode (WE) with a test area of 1.0 cm^2. To ensure a steady state, the working electrode was immersed in the solution for 30 minutes prior to potentiodynamic polarization (PP) measurements.

Potentiodynamic cathodic and anodic polarization curves were obtained by scanning from -0.5 V to +0.5 V versus open circuit potential (OCP) at a scan rate of 5 mV/s. The linear Tafel segments of both the anodic and cathodic curves were extrapolated to the corrosion potential (E_{corr}) to calculate the corrosion current densities (i_{corr}). Inhibition efficiency (η_{IE}) was calculated using i_{corr} values, as shown in Equation (1).

All impedance measurements were performed using AC signals with a 10 mV peak-to--peak amplitude at the steady-state potential, across a frequency range of 10 kHz to 10 mHz. Measurements were conducted for 30 minutes and 24 hours after immersion in the electrolyte. Bode diagrams were generated from these measurements, and EIS parameters obtained by fitting the equivalent circuit were used to calculate the inhibition efficiency using Equation (2).

$$\eta_{IE}(\%) = \left(1 - \frac{i_{corr}\ (inhibitor)}{i_{corr}(uninhibitor)}\right) x\ 100 \quad (1)$$

$$\eta_{IE}(\%) = \left(1 - \frac{R_{ct}\ (uninhibitor)}{R_{ct}\ (inhibitor)}\right) x\ 100 \quad (2)$$

RESULTS AND DISCUSSION

PHYSICAL-CHEMICAL CHARACTERIZATION

Figure 2 shows the results obtained from the physicochemical characterization of the chitosan used in this study.

It is important to note that crystallinity is influenced by several factors, such as the source organism from which chitin is extracted, the conditions used in the polymer extraction process, and the specific steps involved, including demineralization, the degree of deacetylation, and purification of the final product (Andrade et al., 2012). The XRD pattern of chitosan, shown in Figure 2(a), exhibited a semi-crystalline structure, which can be attributed to strong intra- and intermolecular interactions, including hydrogen bonds between amine, alcohol, amide, and other functional groups in the chitosan molecule. Contrary to literature reports that indicate a sharp peak at $2\theta = 20^o$ (Zhang et al., 2005; Dey et al., 2016; Eddya et al., 2020), this peak was not as pronounced in the obtained diffractogram. Other peaks observed ($2\theta = 23.5^o$, 29.8^o, 36.5^o, 39.8^o, 43.5^o, 48^o, and 49.2^o) likely result from incomplete mineral removal from the raw material, as chitosan derived from crabs and other marine crustaceans often contains a high mineral content (30% to 50%), predominantly $CaCO_3$

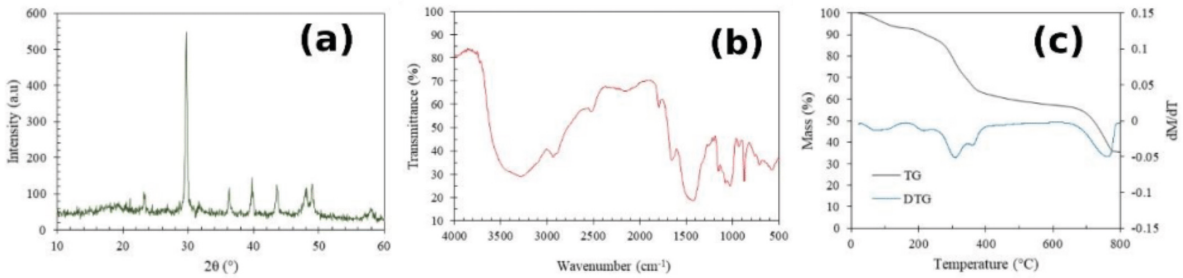

Figure 2 - (a) XRD pattern; (b) FT-IR spectrum and (c) TGA-DTG thermogram of chitosan.

(Hajji et al., 2014; Pellis et al., 2022). Ma et al. (2021) reported similar 2θ peaks when analyzing micro-sized cubic $CaCO_3$ particles.

FT-IR analysis aimed to identify the major functional groups present in chitosan. The FT-IR spectrum of chitosan, Figure 2(b), showed an overlap of the -OH axial stretching and -N-H symmetrical stretching bands in the 3100 cm^{-1} to 3500 cm^{-1} range. Other notable bands included -CH_2 stretching at 2920 cm^{-1}, -C=O amide I acetyl group deformation at 1655 cm^{-1}, and -C-N amide deformation at 1430 cm^{-1}. Bands associated with polysaccharide structures were identified in the 1145 cm^{-1} to 870 cm^{-1} range. The decreased carbonyl intensity at 1655 cm^{-1} could be related to the deacetylation process, as this band tends to diminish with higher deacetylation degrees. Bands near 700 cm^{-1}, 870 cm^{-1}, 1145 cm^{-1}, 1430 cm^{-1}, and 1800 cm^{-1} were consistent with carbonate (CO_3^{2-}) bands reported by Saharudin et al. (2017), confirming the presence of $CaCO_3$ in the sample, as also detected by XRD. This indicates that the chitosan extraction process did not fully demineralize the raw material (crustacean exoskeleton) before deproteinization and deacetylation. Although not of analytical purity, the bands in this spectrum align with those reported in the literature (Parvez et al., 2012; Mauricio-Sánchez et al., 2018; Mubarak et al., 2021).

Thermal degradation and carbonaceous residue formation in chitosan were investigated through thermogravimetric analysis (TGA) and are shown in Figure 2(c). A mass loss stage between 50°C and 140°C, primarily attributed to the loss of water (~10%), bound to amino and hydroxyl groups, was observed. Significant mass reduction occurred between 280°C and 400°C (with maximum degradation at 308°C), corresponding to chitosan degradation and deacetylation through random breaking of glycosidic bonds, vaporization, and elimination of volatile products (Dey et al., 2016), resulting in approximately 45% mass loss. The main degradation temperature of chitosan aligns with previous reports (Jing et al., 2019). The final degradation stage, occurring between 650°C and 800°C, left a solid residue of 35% by mass. This stage is associated with $CaCO_3$ degradation (Ma et al., 2021), consistent with earlier XRD and FT-IR analysis that confirmed the presence of $CaCO_3$ in the commercial chitosan.

The notable thermal degradation observed above 280°C limits the use of this inhibitor in high-temperature systems. Therefore, it is essential to carefully control the operating temperature during its application to avoid compromising its stability and, consequently, its corrosion performance.

CORROSION PERFORMANCE

The PP curves in the absence and presence of chitosan are shown in Figure 2, with the corresponding data provided in Table 2. The inhibitor primarily affected the anodic reaction rather than the cathodic reaction, suggesting that its addition slows down the metal dissolution process. However,

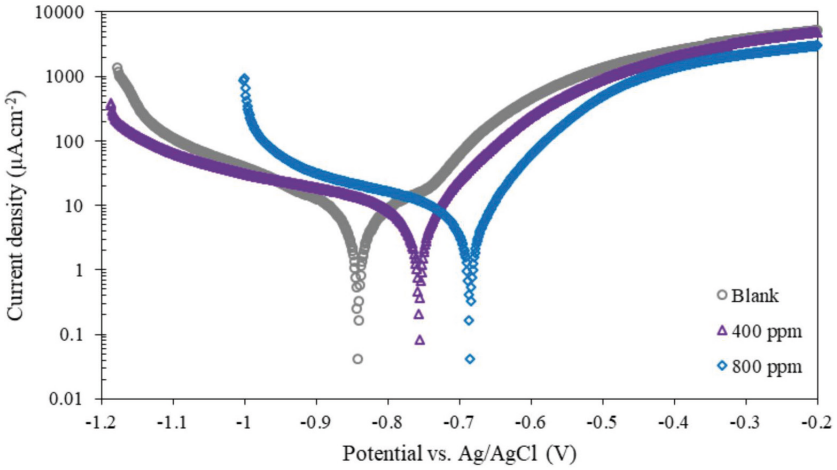

Figure 2 - Potentiodynamic polarization curves for mild steel after 30 min of immersion in 0.1 M NaCl solution solution without (blank) and with 400 ppm and 800 ppm of chitosan

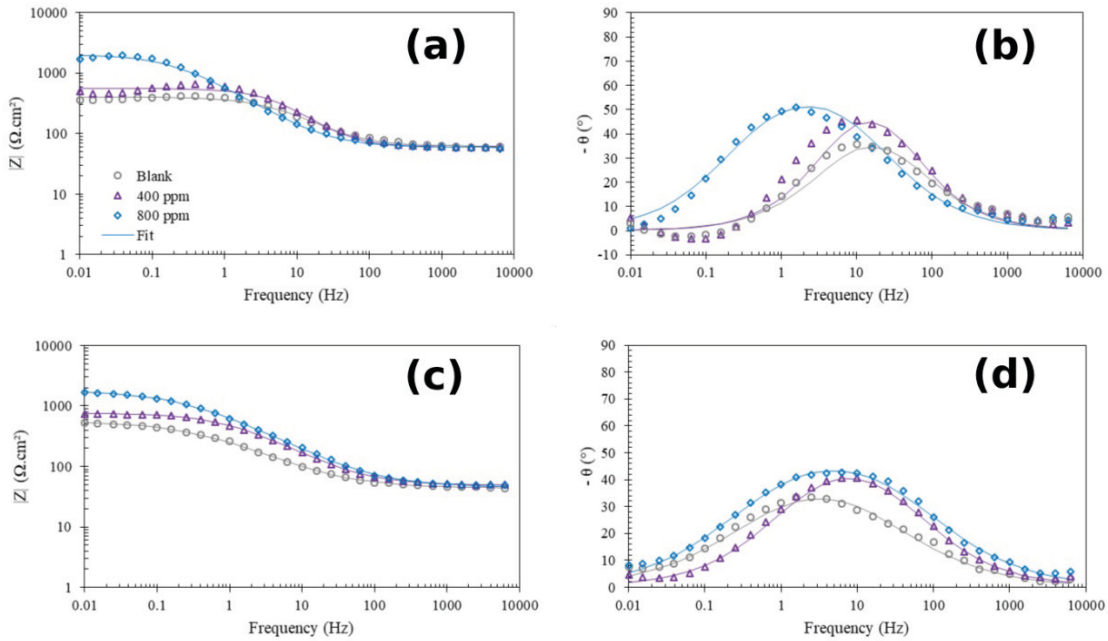

Figure 3 - Bode diagrams for carbon steel in 0.1M NaCl solution without (blank) and with 400 ppm and 800 ppm of chitosan: (a) and (b) after 30 min of immersion; (c) and (d) after 24 h of immersion.

Eletrolyte	Immersion time (h)	R_s (Ω)	R_{ct} (Ω)	CPE (μF)	η_{IE} (%)
0.1 M NaCl (Blank)	0.5	62	339	95	---
0.1 M NaCl + 400 ppm chitosan		60	495	79	31.6
0.1 M NaCl + 800 ppm chitosan		59	1974	370	82.8
0.1 M NaCl (Blank)	24	44	517	759	---
0.1 M NaCl + 400 ppm chitosan		48	714	202	27.5
0.1 M NaCl + 800 ppm chitosan		45	1750	334	70.5

Table 3 – Impedance parameters obtained from the equivalent circuit fitting.

the difference in E_{corr} values reached 150 mV higher in the presence of the inhibitor, indicating that it is predominantly anodic in nature. The efficiency values obtained for 800 ppm (over 70%) are consistent with those reported by other researchers for this polymer (Solomon et al, 2017; Fayomi et al., 2018). The η_{IE} for 800 ppm of chitosan was significantly higher than that for 400 ppm, which may be attributed to a multilayer adsorption mechanism that effectively covers the metal surface, blocking major active sites.

Electrolyte	E_{corr} (V *vs* Ag/AgCl)	i_{corr} (mA. cm^{-2})	η_{IE} (%)
0.1 M NaCl (Blank)	-0.84	6.1	---
0.1 M NaCl + 400 ppm chitosan	-0.76	3.4	44.3
0.1 M NaCl + 800 ppm chitosan	-0.69	1.8	72.1

Table 2 – Potentiodynamic polarization parameters for mild steel in the absence and presence of chitosan.

Bode plots of the EIS results are shown in Figure 3. The equivalent circuit, represented in Figure 4 was used to analyze the electrochemical processes involved, including R_s (solution resistance), R_{ct} (charge transfer resistance) and CPE (constant phase element). The impedance parameters were extracted by fitting the equivalent circuit and the results are summarized in Table 3. R_{ct} values increased with chitosan concentration indicating that the compound acts as an adsorption inhibitor, forming a barrier that impedes mass and charge transfer on the electrode surface. After 24 hours of immersion, the corrosion efficiency decreased due to the penetration of aggressive Cl^- ions through the adsorbed inhibitor layer, which reached the metal surface and initiated localized corrosion.

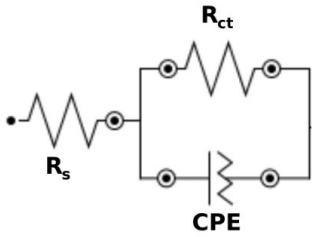

Figure 4 – Equivalent circuit used for fitting experimental EIS data.

CONCLUSIONS

Chitosan is an important class of natural biopolymers with diverse biological and industrial applications. It has also proven to be an environmentally friendly corrosion inhibitor for carbon steel in acidic sodium chloride solutions. Like other natural compounds, chitosan and its derivatives require thorough characterization, as even small changes in their structure and composition can significantly affect their adsorption capacity on metal surfaces, and consequently, their anticorrosive performance. The commercial chitosan used in this study exhibited a semi-crystalline structure, thermal degradation above 280°C, and the presence of mineral impurities such as $CaCO_3$, indicating a low degree of purity due to the raw material and production process. The addition of chitosan to the corrosive medium resulted in a shift of Ecorr toward the noble direction, accompanied by an increase in inhibition efficiency as the concentration of the inhibitor increased. Chitosan acted as an interface-type corrosion inhibitor, adsorbing onto the metal/electrolyte solution interface and effectively preventing corrosion of carbon steel in acidic sodium chloride medium. At 800 ppm, the inhibition efficiency reached over 70%, even after 24 hours of exposure. It is clear that the purity of chitosan, the nature of the metal, the corrosive medium, and the working temperature must all be carefully considered to ensure optimal anticorrosive performance.

REFERENCES

Ashassi-Sorkhabi, H.; Kazempour, A. (2020). Chitosan, its derivatives and composites with superior potentials for the corrosion protection of steel alloys: A comprehensive review. **Carbohydrate Polymers**, 237, 116110.

Andrade, S.M.B.D.; Landchumanandasivam, R.; Rocha, B.G.D.; Belarmino, D.D.; Galvão, A.O. (2012). The use of exoskeletons of shrimp (*Litopenaeus vanammei*) and crab (*Ucides cordatus*) for the extraction of chitosan and production of nanomembrane. **Materials Sciences and Applications**, 3, 495-508.

Ashassi-Sorkhabi, H.; Kazempour, A. (2020). Chitosan, its derivatives and composites with superior potentials for the corrosion protection of steel alloys: A comprehensive review. **Carbohydrate Polymers,** 237, 116110.

Arthur, D.E.; Jonathan, A.; Ameh, P.O.; Anyaet, C. (2013). A review on the assessment of polymeric materials used as corrosion inhibitor of metals and alloys. **International Journal of Industrial Chemistry**, 4:12, 1-9.

Atta, A.M.; El-Mahdy, G.A.; Al-Lohedan, H.A., Ezzat, A.-R.O. (2015). Synthesis of nonionic amphiphilic chitosan nanoparticles for active corrosion protection of steel. **Journal of Molecular Liquids**, 211, 315–323.

Carneiro, J.; Tedim, J, Ferreira, M.G.S. (2015). Chitosan as a smart coating for corrosion protection of aluminum alloy 2024: A review. **Progress in Organic Coatings**, 89, 348–356.

Dahmane, E.M.; Taourirte, M.; Eladlani, N.; Rhazi. M. (2014). Extraction and Characterization of Chitin and Chitosan from *Parapenaeus longirostris* from Moroccan Local Sources. **International Journal of Polymer Analysis and Characterization**, 19, 342-351.

Dey, S.C.; Al-Amin, M.; Rashid, T.U.; Sultan, M.Z.; Ashaduzzaman, M.; Sarker, M.; Shamsuddin, S.M. (2016). Preparation, characterization and performance evaluation of chitosan as an adsorbent for remazol red. **International Journal of Latest Research in Engineering and Technology**, 2, 52-62.

Du, DX; Vuong, B.X. (2019). Study on Preparation of Water-Soluble Chitosan with Varying Molecular Weights and Its Antioxidant Activity. **Advances in Materials Science and Engineering**, 1-8.

Eddya, M.; Tbib, B.; EL-Hami, K. (2020). A comparison of chitosan properties after extraction from shrimp shells by diluted and concentrated acids, **Heliyon**. 6, 1-17.

El-shamy, H.F.M.; Aggour, Y.A.; El-batouti, M., A. M. Ahmed, A.M. (2017). Electropolishing of carbon steel in presence of some natural polymers under natural and forced convection conditions. **International Journal of Advanced Research in Chemical Science**, 4, 1-12.

Faccini, M.; Bautista, L.; Soldi, L.; Escobar, A.M.; Domènech, A.; Domínguez, E. (2021). Environmentally Friendly Anticorrosive Polymeric Coatings. **Applied Sciences**, 11, 3446.

Farag, A.A.; Al-Shomar, S.M.; Abdelshaf, N.S. (2024). Eco-friendly modifed chitosan as corrosion inhibitor for carbon steel in acidic medium: Experimental and in-depth theoretical approaches. **International Journal of Biological Macromolecules**, 279, 135408.

Fayomi, O.S.I.; Akande, I.G.; Oluwole, O.O.; Daramola, D. (2018). Effect of water-soluble chitosan on the electrochemical corrosion behaviour of mild steel. **Chemical Data Collections**, 17/18, 321-326.

Hajji, S.; Younes, I.; Ghorbel-Bellaaj, O.; Hajji, R.; Rinaudo, M.; Nasri, M.; Jellouli, K. (2014). Structural differences between chitin and chitosan extracted from three different marine sources. **International Journal of Biological Macromolecules**, 65, 298–306.

Hasanin, M.; Al Kiey, S.A.; (2023). Development of ecofriendly high performance anti-corrosive chitosan nanocomposite material for mild steel corrosion in acid medium. **Biomass Conversion and Biorefnery**, 13,12235–12248.

Hossain, N.; Chowdhury, M.A.; Kchaou, M. (2020). An overview of green corrosion inhibitors for sustainable and environment friendly industrial development. **Journal of Adhesion Science and Technology**, 1-20.

Jing. Y.; Diao. Y.; Yu. X. (2019). Free radical-mediated conjugation of chitosan with tannic acid: Characterization and antioxidant capacity, **Reactive and Functional Polymers**, 135, 16-22.

Kumar, A.M.; Rajesh, T.; Obot, I.B.; Sharfan, I.I.B.; Abdulhamid, M.A. (2024). Water-soluble chitosan salt as ecofriendly corrosion inhibitor for N80 pipeline steel in artifcial sea water: Experimental and theoretical approach. **International Journal of Biological Macromolecules**, 254, 127697.

Lai, X.; Hu, J.; Ruan, T.; Zhou, J.; Qu, J. (2021). Chitosan derivative corrosion inhibitor for aluminum alloy in sodium chloride solution: A green organic/inorganic. **Carbohydrate Polymers**, 265, 118074.

Ma, Y.; Tian, P.; Bounmyxay, M.; Zeng, Y.; Wang, N. (2021). Calcium Carbonate@silica Composite with Superhydrophobic Properties. **Molecules,** 26, 7180, 1-14.

Marzorati, S.; Verotta, L.; Trasatti, S. (2019). Green Corrosion Inhibitors from Natural Sources and Biomass Wastes, **Molecules,** 24, 1-24.

Mauricio-Sánchez. R.A.; Salazar R.; Luna-Bárcenas, J.G.; Mendoza-Galván. A. (2018). FTIR spectroscopy studies on the spontaneous neutralization of chitosan acetate films by moisture conditioning, **Vibrational Spectroscopy,** 94, 1–6.

Mubarak, M.F.; Ragab, A.H.; Hosny, R.; Ahmed, I.A.; Ahmed, H.A.; EL-Bahy. S.M.; Shahawy, A.E. (2021). Enhanced performance of chitosan via a Novelquaternary magnetic nanocomposite chitosan/grafted halloysitenanotubes@ Zn$\gamma$$Fe_3O_4$ for uptake of Cr (III), Fe (III), and Mn (II) from wastewater, **Polymer,** 13, 1-19.

Okoronkwo, A. E.; Olusegun, S.J.; Oluwasina, O.O. (2015). The inhibitive action of chitosan extracted from Archachatina marginata shells on the corrosion of plain carbon steel in acid media. **Anti-Corrosion Methods and Materials**, 62:1,13-18.

Oyekunle, D.T.; Agboola, O.; Ayeni, A.O. (2019). Corrosion inhibitors as building evidence for mild steel: A review. **Journal of Physics: Conference Series**, 1378, 1-23.

Parvez, S.; Rahman, M.M.; Khan, M.A.; Khan, M.A.H.; Islam, J.M.M.; Ahmed, M.; Ahmed, B. (2012). Preparation and characterization of artificial skin using chitosan and gelatin composites for potential biomedical application, **Polymer Bulletin,** 69, 715-731.

Pellis, A.; Guebitz, G.M.; Nyanhongo, G.S. (2022). Chitosan: Sources, Processing and Modification Techniques. **Gels**, 8:393, 1-27.

Rabizadeh, T.; Asl, S.K. (2018). Chitosan as a green inhibitor for mild steel corrosion: Thermodynamic and electrochemical evaluations. **Materials and Corrosion**,1–11.

Raja, P.B.; Fadaeinasab, M.; Qureshi, A.K.; Rahim, A.A.; Osman, H.; Litaudon, M.; Awang, K. (2013). Evaluation of Green Corrosion Inhibition by Alkaloid Extracts of Ochrosia oppositifolia and Isoreserpiline against Mild Steel in 1 M HCl Medium**. Industrial & Engineering Chemistry Research,** 52:31, 10582-10593.

Saharudin, S.H.; Shariffuddin, J.H.; Nordin, N.I.A.A. (2017). Biocomposites from (*Anadara granosa*) shells waste for bone material applications**, IOP Conference Series: Materials Science and Engineering,** 257, 1-10.

Solomon, M.M.; Gerengi, H.; Kaya, T.; S.A. Umoren, S.A.. (2017). Enhanced corrosion inhibition effect of chitosan for St37 in 15% H_2SO_4 environment by silver nanoparticles. **International Journal of Biological Macromolecules**, 104, 638-649.

Umoren. S. A, Solomon. M. M. (2014). Recent development on the use of polymers as corrosion inhibitors: A review. **Open Material Sciences**, 8, 39-54.

Verma, C.; Kumar, A.D.; Mazumber, M.A.J.; Quraishi, M.A. (2018). Chitosan-based green and sustainable corrosion inhibitors for carbon steel. **Chitin-Chitosan - Myriad Functionalities in Science and Technology**, ed. R.S. Dongre, InTech, 2018. Available from: http://dx.doi.org/10.5772/intechopen.71146Chitin-Chitosan: Myriad Functionalities in Science and Technology.

Zhang, Q.H.; Xu, N.; Jiang, Z.N.; Liu, H.F.; Zhang, G.A. (2023). Chitosan derivatives as promising green corrosion inhibitors for carbon steel in acidic environment: Inhibition performance and interfacial adsorption mechanism. **Journal of Colloid and Interface Science**, 640, 1052–1067.

Zhang, Y.; Xue, C.; Xue, Y.; Gao, R.; Zhang, X. (2005). Determination of the degree of deacetylation of chitin and chitosan by X-ray powder diffraction, **Carbohydrate Research,** 340, 1914-1917.

Zhen, D.; Zhang, S.; Zhang, X.; Zhang, H.; Wang, J.; Chen, B.; Liu, Y.; Luo, X. (2023). Natural chitosan-based carbon dots as an eco-friendly and effective corrosion inhibitor for mild steel in HCl solution. **International Journal of Biological Macromolecules**, 253, 126449.